To appear in ASME Letters in Dynamic Systems and Control

Early Detection of Fatigue Crack Damage in Ductile Materials: A Projection-based Probabilistic Finite State Automata Approach

Chandrachur Bhattacharya
Departments of Mechanical and Electrical Engineering
Pennsylvania State University
University Park, PA 16802
Email: chandrachur.bhattacharya@gmail.com

Susheel Dharmadhikari
Department of Mechanical Engineering
Pennsylvania State University
University Park, PA 16802
Email: sud85@psu.edu

Amrita Basak
Department of Mechanical Engineering
Pennsylvania State University
University Park, PA 16802
Email: aub1526@psu.edu

Asok Ray, Fellow ASME
Departments of Mechanical Engineering and Mathematics
Pennsylvania State University
University Park, PA 16802
Email: axr2@psu.edu

Abstract

Fatigue failure occurs ubiquitously in mechanical structures when they are subjected to cyclic loading well below the material's yield stress. The tell-tale sign of a fatigue failure is the emergence of cracks at the internal or surface defects. In general, a machinery component has a finite fatigue life based on the number of cycles it can sustain before a fracture occurs. However, the estimated life is generally conservative and often a large factor of safety is applied to make the component fail-safe. From the perspective of better utilization of a machinery component, it is, however, desirable to have maximum usage of the component without a catastrophic failure. It is, therefore, conducive to have a measure that can capture precursors to failure to facilitate active diagnosis of the machinery health. In this letter, a precursor detection method is developed upon modifications of probabilistic finite state automata (PFSA). The efficacy of the proposed method is demonstrated on cold-rolled AL7075-T6 notched specimens in a computer-instrumented and computer-controlled fatigue testing apparatus. The results show that the proposed method is capable of detecting the emergence of cracks (at $\sim 95\%$ *accuracy) and also can capture precursors with good fidelity.*

Keywords: Polycrystalline aluminum alloy; Fatigue damage; Early detection; Probabilistic finite state automata (PFSA).

1 Introduction

Prediction of structural damage and estimation of remaining useful life (RUL) are both critical for safe, reliable, and cost-effective operation of mechanical systems that typically experience fatigue damage during both nominal and off-nominal operations [1]. Early detection of fatigue damage not only averts catastrophic failures but also facilitates predictive maintenance strategies with a significant reduction of the life cycle cost. In the current state-of-the-art, while direct measurement of fatigue damage at an early stage (e.g., crack initiation) is possible using sophisticated custom-designed fatigue stages inside computed tomography equipment, such measurement techniques may not be readily deployed on operating machinery. An alternative is to use advanced computational modeling; however, prediction of fatigue damage evolution is often intractable through the sole usage of computational models, because such models grossly approximate the mechanisms of surface deformation, surface energy, stacking fault energy, and anti-phase boundary energy. These approximations result in a non-robust estimation of cyclic strain accumulation, crack initiation, and small crack propagation. Furthermore, since the operating environment may change continuously, it is very difficult to accurately predict the fatigue life of machinery *a-priori*.

One of the logical alternatives, therefore, is to employ an online anomaly detection framework that will continuously monitor the machinery health and alert the user of an impending failure. To handle the challenge of online monitoring using field-deployable sensors, low-cost sensing methods (e.g., ultrasonic, acoustic emission, and eddy current) have been reported in literature [2, 3]. Amongst all these techniques, ultrasonic transducers (UT) are widely used in industry, because they are responsive to small microstructural changes in early stages of fatigue damage [4]. Tools of statistical pattern recognition, time-series analysis, and wavelet-based feature detection, thereafter, can be applied on UT data for online health monitoring in critical components [4, 5].

The current paper reports major modifications of the standard probabilistic finite state automata (PFSA) [4, 6]

method, where the objective is to detect the emergence of an imminent fatigue crack by using the ultrasonic data as described above. This is done by computing a scalar-valued function that denotes the structural health (i.e., fatigue crack damage) of the specimen and the discrimination is accomplished using a thresholded approach.

Contributions: Major contributions of the work reported in this letter are as follows.

1. *Modifications of the standard PFSA formulation* [4, 6]: These modifications alleviate some of the inherent drawbacks in the original formulation [4]. An example is orthogonal projection of the probability state vector, constructed from a test time series, onto feature spaces corresponding to different regimes. Another example is related to data normalization prior to partitioning, which allows the signal texture to be retained, but not necessarily the signal values.
2. *Validation of the proposed crack detection method*: The efficacy of the detection method is demonstrated on an experimental apparatus to perform classification of uncracked and cracked specimens under cyclic load as well as to capture precursors for early detection of imminent crack appearance.

Organization: The letter is organized in six sections including the present one. Section 2 introduces the mathematical background for the reported work. Section 3 develops the proposed method of PFSA-based projection for classification. Section 4 describes the experimental apparatus and develops the fatigue crack detection algorithm. Section 5 presents and discusses the results of experimental validation of the fatigue crack detection method. Section 6 summarizes and concludes the reported work along with a few recommendations for future research.

2 Mathematical background

While the details are available in current literature (e.g., [6–9]), this section presents a very brief background for the work reported in this letter.

2.1 Introduction to Probabilistic Finite State Automata

Probabilistic finite state automata (PFSA) are constructed by first symbolizing (quantizing) time-series data with the usage of a partitioning scheme [8]. This procedure converts a continuous-valued time series into a discretized string of symbols from an alphabet, where the cardinality of the alphabet is equal to the number of cells used for quantization.

Definition 1. *A finite state automaton (FSA) G, having a deterministic algebraic structure, is a triple $(\mathcal{A}, Q, \delta)$ where:*

- *$\mathcal{A}$ is a (nonempty) finite alphabet, i.e., its cardinality $|\mathcal{A}|$ is a positive integer.*
- *Q is a (nonempty) finite set of states, i.e., its cardinality $|Q|$ is a positive integer..*
- *$\delta : Q \times \mathcal{A} \to Q$ is a (deterministic) state transition map.*

Definition 2. *A probabilistic finite state automaton (PFSA), J, is a pair $J = (G, \pi)$, where:*

- *The deterministic FSA, G, is called the underlying FSA of the PFSA, J.*
- *The probability map, $\pi : Q \times \mathcal{A} \to [0, 1]$, is called the morph function (also known as symbol generation probability function) that satisfies the condition: $\sum_{s \in \mathcal{A}} \pi(q, s) = 1$ for each $q \in Q$. The map, π, can be represented by a $|Q| \times |\mathcal{A}|$ stochastic matrix, Π, (i.e., each element of Π is non-negative and each row sum of Π is unity). In that case, the PFSA is a quadruple, i.e., $J = (\mathcal{A}, Q, \delta, \Pi)$.*
- *The state transition probability mass function, $\tau : Q \times Q \to [0, 1]$, is constructed by combining δ and Π, which can be structured as a $|Q| \times |Q|$ state transition probability matrix, T. In that case, the PFSA can also be described as a triple, i.e., $J = (\mathcal{A}, Q, T)$.*

Remark 3. *Prior to partitioning, the time series is normalized to be either zero-mean and unit-variance, or to unit-range. The rationale for normalization is to mitigate the effects of bias and spurious noise in the time series and to ensure that a fixed set of partition boundaries can be used across the full range of data. The fixed partitioning allows comparison of different PFSAs as they evolve and also eliminates the need to recompute the partitioning during testing. Details are given in Subsection 3.2.*

2.2 *D*-Markov Machines

The PFSA structure of a D-Markov machine generates symbol strings $\{s_1 s_2 \cdots s_\ell : s_j \in \mathcal{A}$ and ℓ is a positive integer$\}$ on the underlying Markov process. In the construction of a D-Markov machine, it is assumed that the generation of the next symbol has a dependence only on a *finite* history of the last D or less consecutive symbols, i.e., the (most recent) symbol block of length not exceeding D. A D-Markov machine [6] is defined as follows.

Definition 4. *A D-Markov machine [7] is a PFSA in the sense of Definition 2 and it generates symbols that solely depend on the (most recent) history of at most D consecutive symbols, where the positive integer D is called the depth of the machine. Equivalently, a D-Markov machine is a statistically stationary stochastic process $S = \cdots s_{-1} s_0 s_1 \cdots$, where the probability of occurrence of a new symbol depends only on the last consecutive (at most) D symbols, i.e.,*

$$P[s_n \mid \cdots s_{n-D} \cdots s_{n-1}] = P[s_n \mid s_{n-D} \cdots s_{n-1}]$$

Remark 5. *If the depth of the D-Markov machine is unity (i.e., $D = 1$), then the state set, Q, and symbol alphabet, $\mathcal{A}$, become equivalent, i.e., the morph matrix, Π and the state transition probability matrix, T are identical if $D = 1$.*

The maximum possible number of states is fixed to $|\mathcal{A}|^D$ once the alphabet size, $|\mathcal{A}|$, and depth, D, are set. To generate the the morph matrix, Π, from a (finite-length) symbol string, S, the occurrence of each state is sequentially counted. Let N_{ij} denote the number of times the symbol $\mathcal{A}_j \in \mathcal{A}$ is emitted from the state $q_i \in Q$. Thus,

$$\Pi_{ij} = \pi(q_i, s_j) \triangleq \frac{1 + N_{ij}}{|\mathcal{A}| + \sum_{\ell} N_{i\ell}} \tag{1}$$

Initializing the count of each element to 1 ensures that, if no event is generated at a state $q \in Q$, there should be no preference to any particular symbol, making it logical to have $\pi(q, s) = 1/|\mathcal{A}| \; \forall s \in \mathcal{A}$, i.e., the uniform distribution of event generation at the state, q. This procedure guarantees that the PFSA, constructed from a (finite-length) symbol string, must have an (element-wise) strictly positive morph map, Π. This also ensures ergodicity and stochasticity of the morph matrix, Π, by construction.

Remark 6. *The mathematical logic used to generate the morph matrix, Π, and state transition probability matrix, T, guarantees that these matrices are both stochastic (i.e., each matrix element is non-negative and each row sum is unity [10]) and ergodic (i.e. every state of the PFSA can be reached in a finite number of iterations irrespective of the starting state [5, 10]). These matrix properties of stochasticity and ergodicity are necessary for the development of the mathematical theory of the modified method of PFSA-based classification, presented in this letter.*

3 PFSA-based Projection for Classification

This section develops the proposed method of PFSA-based projection, hereafter called *p-PFSA*. The state probability vector of the PFSA is projected onto the feature hyperplanes corresponding to different operating regimes of the dynamical system. The theme of constructing the proposed *p-PFSA* is presented below.

Let $T \in \mathbb{R}^{n \times n}$, where n is a positive integer, be an ergodic stochastic matrix [10]. Ergodicity of the stochastic matrix, T, implies the existence of exactly one eigenvalue, $\lambda_0 = 1$ and the remaining $m \leq (n-1)$ distinct eigenvalues are located on or inside the unit circle (with center at 0) in the complex plane, i.e., $|\lambda_i| \leq 1$ for $i = 1, 2, \cdots, m$. If some of the eigenvalues are repeated, it is possible that there will be only m linearly independent left eigenvectors, $v_1', \cdots, v_m'$ and m linearly independent right eigenvectors , $u_1, \cdots, u_m$, where $1 \leq m \leq (n-1)$. Each of these eigenvectors could be normalized and ordered for convenience as follows.

$$1 \geq |\lambda_1| \geq \; \cdots \; \geq |\lambda_m| \geq 0$$

It is noted that these eigenvalues are either real or pairs of complex conjugates and their respective left eigenvectors, $\{v_i'\}$, and right eigenvectors, $\{u_i\}$, are also either real or pairs of complex conjugates as seen below.

$$v_i' T = \lambda_i v_i' \implies \bar{v}_i' T = \bar{\lambda}_i \bar{v}_i' \;\text{ and }\; T u_i = \lambda_i u_i \implies T \bar{u}_i = \bar{\lambda}_i \bar{u}_i$$

where $\bar{v}_i$, $\bar{u}_i$ and $\bar{\lambda}_i$ are complex conjugates of v_i, u_i and λ_i, respectively. Let v_0' and u_0 be respectively the (normalized) left and right eigenvectors of T with respect to the unique eigenvalue, $\lambda_0 = 1$. The remaining left and right eigenvectors are v_i' and u_i, respectively, corresponding to distinct eigenvalues, λ_i.

Claim: *For distinct eigenvalues $\lambda_i \neq \lambda_j$, $(i \neq j)$, $i, j \in \{0, 1, \cdots, m\}$, the inner product $\langle v_i, u_j \rangle = 0$, i.e., $v_i \perp u_j$.*

Justification of Claim:

Since $\lambda_i \neq \lambda_j$, at least one of them is non-zero. Without loss of generality, one may set $\lambda_i \neq 0$. Then,

$$\langle v_i, u_j \rangle = v_i' u_j = \frac{1}{\lambda_i} v_i' T u_j = \frac{\lambda_j}{\lambda_i} v_i' u_j = \frac{\lambda_j}{\lambda_i} \langle v_i, u_j \rangle$$
$$\implies \left(1 - \frac{\lambda_j}{\lambda_i}\right) \langle v_i, u_j \rangle = 0.$$

Since $\lambda_i \neq \lambda_j$, it follows that $\left(1 - \frac{\lambda_j}{\lambda_i}\right) \neq 0 \implies \langle v_i, u_j \rangle = 0$.

End of Justification

From the above claim, it is concluded that $v_0 \perp u_j$ corresponding to the eigenvalues, λ_j, $j \in \{1, 2, \cdots, m\}$. Therefore, in the training phase, v_0 and $u_j \; \forall j \in \{1, \cdots, m\}$ are identified. In the testing phase, it is necessary to identify only v_0^{tst} (corresponding to an observed test time series belonging to an unknown class) for detection and classification of anomalous events, if any. If there is no anomaly, the vector, v_0^{tst} should be nearly coincident with v_0 and, thus, nearly orthogonal to the m-dimensional subspace spanned by u_j, $j \in \{1, 2, \cdots, m\}$, which has already been identified in the training phase. However, in the presence of an anomaly, v_0^{tst} should very likely deviate from v_0 that corresponds to the nominal phase.

The key idea behind the development of *p-PFSA* is to quantify the anomaly as a deviation of v_0^{tst} from v_0 by using the projection of v_0^{tst} onto the space spanned by $u_j \; \forall j = 1, \cdots, m$. From the perspectives of energy distribution, the absolute values, $|\lambda_i|$, of the eigenvalues signify the energy associated with the (normalized) eigenvector u_i; therefore, each u_i, $i = 1, \cdots, m$ is weighted as $\sqrt{|\lambda_i|}\, u_i$. The normalized version of $\sqrt{|\lambda_i|}\, u_i$ is u_i, because the u_i's were originally generated as normalized vectors.

For a general ergodic stochastic matrix T, the right eigenvectors may not be orthogonal to each other. Therefore, the (linearly independent) vectors $\sqrt{|\lambda_i|}\, u_i$, $i = 1, \cdots, m$, are further transformed by Gram-Schmidt orthogonalization as a set of mutually orthogonal vectors $\tilde{u}_i, i = 1, \cdots, m$, i.e., $\langle \tilde{u}_i, \tilde{u}_j \rangle = 0 \; \forall i \neq j$. Having identified the m mutually orthogonal n-dimensional vectors $\tilde{u}_i$, the n-dimensional weighted error vector, $\mathcal{E}$, is obtained by projection of the vector v_0^{tst} onto the m-dimensional subspace, spanned by $\tilde{u}_i$, $i = 1, \cdots, m$, where $1 \leq m \leq (n-1)$, as:

$$\mathcal{E} \triangleq \sum_{i=1}^{m} \langle v_0^{tst}, \tilde{u}_i \rangle u_i \quad \text{with } ||\mathcal{E}|| \; = \sqrt{\sum_{i=1}^{m} |\langle v_0^{tst}, \tilde{u}_i \rangle|^2} \tag{2}$$

3.1 The PFSA-based Projection Algorithm: *p-PFSA*

This subsection addresses a classification problem with a total number of C classes (i.e., regimes). In the training phase, a PFSA is generated for each class as described in Subsection 2.1. The state transition probability matrix, T^c of each class, $c \in \{1, 2, \cdots, C\}$ is treated as the feature for the respective class (i.e., regime). In this letter, T^c is equivalent to Π^c because the PFSA is constructed with $D = 1$ (see Remark 5), and each T^c is ergodic and stochastic (see Remark 6); therefore, for each T^c, there exists a set of orthogonalized right eigenvectors, $\{\tilde{u}_i^c\}$, where for each class

$c, i = 1, \cdots, m^c$, and $1 \leq m^c \leq (n-1)$ is the number of linearly independent eigenvectors for class c. Each set of orthogonalized right eigenvectors, $\{\tilde{u}_i^c\}$, generates a hyperplane of dimension, m^c, respectively. It is expected that, for different classes representing distinct operational regimes, the hyperplanes will be distinct. That is, a hyperplane belonging to class, c, will have its distinct normal direction, v_0^c. Classes that are close to each other will have directions close to each other, but they are still expected to be distinct.

In the testing (i.e., classification) phase, a time series is observed, which belongs to an unknown class. The (stochastic and ergodic) state transition probability matrix, T^{tst}, is generated for this time series, and the left eigenvector $(v_0^{tst})'$ of the T^{tst}-matrix is obtained corresponding to the unique eigenvalue $\lambda_0^{tst} = 1$. Then, v_0^{tst} is projected onto each of the C hyperplanes that are generated in the training phase; and the norm of the error vector in each hyperplane is computed as $||\mathcal{E}^c||$, where $c = 1, \cdots, C$. The class corresponding to the lowest error magnitude is identified to be the class to which the testing time series belongs, i.e.,

$$\text{Selected Class} = \underset{c \in \{1,2,\cdots,C\}}{\text{argmin}} \; ||\mathcal{E}^c|| \tag{3}$$

3.2 Modification of Time Series Normalization

As described in Remark 3, prior to partitioning and symbolization, the numerical (i,e., real-valued) time-series is typically normalized, which also allows a fixed set of *global* finitely many partitioning boundaries to be applicable across all data in the classification problem, where each of the data set might have different maximum and minimum values. A common way of data normalization is to have zero mean and unit variance of the data, which unfortunately removes the information of the signal magnitude while retaining only the information about the signal texture (i.e., waveform), as seen in Figure 1. The three plates in the top row of Figure 1 display three sinusoidal signals having identical frequencies but different means and amplitudes; and the three plates in the bottom row show the equivalent normalized signals that are identical and hence indistinguishable. This implies that the PFSAs constructed from these normalized signals will also be (almost) identical. Therefore, it would be impossible for the standard PFSA approach to distinguish between these three signals although the original signals could be significantly different, as seen in the top row of Figure 1.

In this letter, the authors propose a modification to solve the above problem by retaining the numerical values of the signal magnitudes to a large extent. This is accomplished by storing the mean and standard deviation of the raw signal (i.e., original time series) for each of the C classes, namely μ^c and σ^c for $c = 1, \cdots, C$, along with the (PFSA) features. Subsequently, during testing, the mean and standard deviation of the observed data are also computed (μ^{tst} and σ^{tst}). Thus, Eq. (3) is modified as:

$$\text{Class} = \underset{c \in \{1,2,\cdots,C\}}{\text{argmin}} \left\| (\mathcal{E}^{tst,c}, \mu^{tst}, \sigma^{tst}) - (0, \mu^c, \sigma^c) \right\| \tag{4}$$

where each PFSA observation is now augmented to a triplet that includes the entries of the mean (μ) and standard deviation (σ) of the signal both during training and testing. It is noted that $\mathcal{E}^{tst,c}$ denotes the error for projecting the left eigenvector of the observed data on the hyperplane of class, c. The corresponding left hand entry in the second term of Eq. (4) is 0, because the projection of an eigenvector on the hyperplane of the same class is 0, as described in Subsection 3.1.

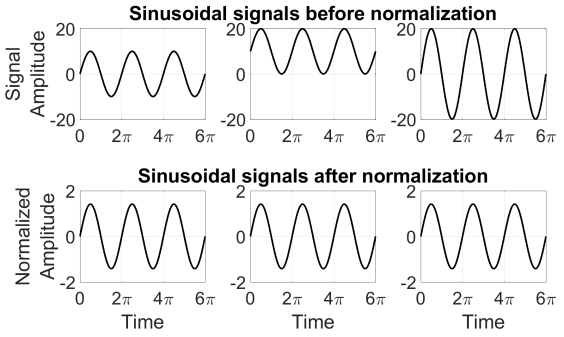

Fig. 1: Zero-mean, unit-variance data normalization
(top row) signals prior to normalization;
(bottom row) signals after normalization

4 Experimental Procedure and Algorithm Development

This section describes the experimental procedure and develops the fatigue crack detection algorithm. Experiments were designed to validate the algorithm; and these experiments have been conducted on a computer-instrumented and computer-controlled fatigue testing apparatus[1] (see Figure 2a) using notched AL7075-T6 specimens (see Figure 2b). Each of the specimens is 3 mm thick with a 50 mm wide gauge section, where the flanges with 3 holes on both ends are 76.5 mm wide and were designed to fix the specimens on the test apparatus by using custom grips.

During the tests, 17 specimens were subjected to a constant-amplitude sinusoidal tensile loading at a frequency of 50 Hz with a mean force of 9,000 N and an amplitude of 1,000 N, which results in a nominal mean stress of 86.5 MPa and a stress amplitude of 9.5 MPa in the specimens. The same load amplitude and frequency were used for all data. To enable early detection of fatigue crack damage, the specimens were fitted with transmitters and receivers of ultrasonic transducers[2] (see Figure 2b). Such transducers are capable of detecting subtle changes in the material impedance due to the ensuing fatigue damage long before any visible crack propagation is noticed.

The sensor outputs, which encode the information about specimen damage, are stored as time-series data for early detection of fatigue damage. Moreover, the test apparatus in Figure 2a is equipped with a travelling digital optical microscope[3] that captures images near the notch base at regular intervals. These images provide visual evidence of the onset of crack formation and are used to corroborate the corresponding temporal location in the ultrasonic signals.

A sample time-series of the ultrasonic signal is provided

[1] Manufacturer: MTS Systems Corporation, Berlin, NJ, USA
[2] Manufacturer: OLYMPUS, Shinjuku, Tokyo, Japan
[3] Manufacturer: QUESTAR®, New Hope, Pennsylvania, USA

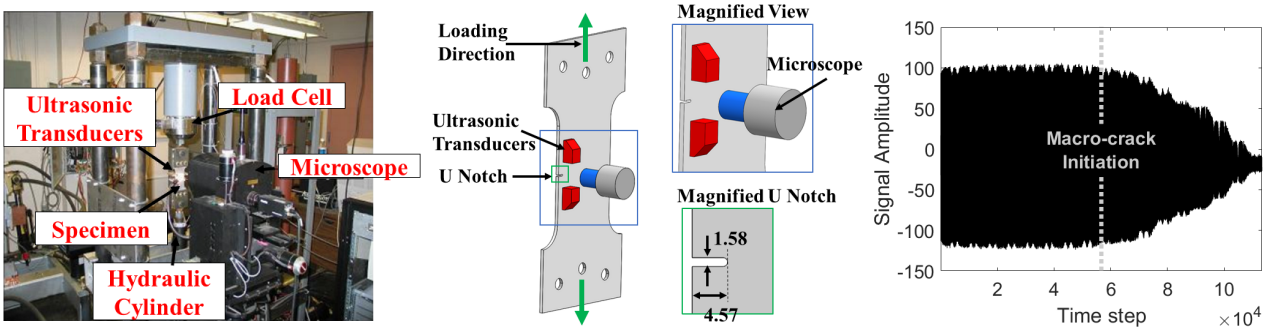

(a) Fatigue testing apparatus, equipped with ultrasonic transducers and a digital microscope

(b) AL7075-T6 U-notched specimen, ultrasonic transducers and microscope. All dimensions are in mm (not to scale)

(c) A typical ultrasonic time-series signal showing crack initiation point as observed by the microscope

Fig. 2: Operational schematic diagram of the computer-instrumented and computer-controlled fatigue testing apparatus

in Figure 2c to illustrate the texture of the signal dynamics. The vertical dotted line denotes the location of the temporal point at which the crack is observed by the microscope; signals to left and right of the point of macro-crack initiation are defined as uncracked and cracked regimes, respectively. The amplitude and texture of the ultrasonic signal are functions of the applied load but (possibly) not the frequency.

4.1 Algorithm for Detection of Fatigue Crack Damage

In the proposed *p-PFSA* method, PFSA models are trained for two classes, namely, *uncracked* (i.e., prior to cracks observed by the optical microscope) and *cracked*. This training is done using 13 specimen time-series (i.e., $\sim 65\%$ of the available data) in each trial, and the remaining 4 specimen time-series are used for testing. Since a thresholded approach has been chosen, the final decision-making during testing is done by modifying Eq. (4). A single scalar-valued metric, ρ, is computed by considering two types of error that are computed in terms of the difference of the observed testing regime from the (trained) uncracked and cracked regimes. Furthermore, the error in the cracked regime is weighted more heavily than that for the uncracked regime, because the objective here is to capture a change into the cracked regime early and, therefore, magnifying the error by a weight w (where $w > 1$) for the cracked regime would help identify the change promptly. To this end, the (signed) measure ρ is defined as:

$$\rho \triangleq \left\| (\mathcal{E}^{tst,\text{uncrack}}, \mu^{tst}, \sigma^{tst}) - (0, \mu^{\text{uncrack}}, \sigma^{\text{uncrack}}) \right\| - w \times \left\| (\mathcal{E}^{tst,\text{crack}}, \mu^{tst}, \sigma^{tst}) - (0, \mu^{\text{crack}}, \sigma^{\text{crack}}) \right\| \quad (5)$$

where the weight is chosen to be $w = 10$ in this letter.

The next step is to identify an appropriate threshold [11] for ρ to discriminate between the uncracked and cracked regimes. The optimal threshold is obtained by using receiver operating characteristic (ROC) curves [12], where the measure ρ yields the lowest total error (false-alarm & missed detection) for training and is set as the optimal threshold (θ) for discrimination of the uncracked and cracked regimes.

By construction of the algorithm, ρ remains near its peak value until just before the crack begins to appear (i.e. when the specimen is still uncracked) and ρ begins decreasing thereafter. The true point of crack appearance is estimated by the microscope as described in Section 4, which is used to learn the threshold parameter θ that can serve as a metric for discriminating between a uncracked and cracked specimen.

Although the terms in the time-series of the (computed) measure ρ are largely similar in the uncracked regime for each specimen, the exact magnitudes may not always match. In order to facilitate the usage of a common threshold across all specimens, the terms in the time-series of ρ are normalized by the average of its values over the first several cycles (e.g., 5,000 time-steps in this letter). During this time span, the specimen is expected not to have any cracks. This process ensures that the range of ρ has a maximum value of ~ 1.

5 Results and Discussions

This section presents and discusses the results of experimental validation of the proposed fatigue crack detection method *p-PFSA*. As described in Subsection 4.1, each train-test trial consists of splitting the available ultrasonic signal time series data of the 17 specimens into a 65-35 split (13 time-series for training the uncracked and cracked regimes, and 4 for testing). To study the average performance of the crack detection algorithm, the confusion matrix for classification between the uncracked and cracked regimes is presented in Table 1, where the results are averaged over 20 individual trials; in each of these cases, the train-test split is done randomly to remove any possible bias. The time series data are first downsampled by a factor of 2 and then are averaged with a window length of 600 data points and a window shift of 100 points. The *p-PFSA* models are trained for both uncracked and cracked regimes with an alphabet size ($|\mathcal{A}|$) of 10, and depth (D) of 1 as discussed in Remark 5. The average error of classification is $\sim 5\%$, as seen in Table 1.

Table 1: Confusion Matrix showing the average classification accuracy of the proposed algorithm

	Classified Uncracked	Classified Cracked
Truly Uncracked	**94.74%**	5.26%
Truly Cracked	3.15%	**96.85%**

The optimal threshold (θ) is seen to have a value of ~ 0.90 on average. By construction, during the uncracked

regime, the measure $\rho \approx 1$; hence, the other fixed early detection threshold parameter is set as $\tilde{\theta} = 0.95$. Since there is no particular ground truth related to emergence of any precursor, $\tilde{\theta}$ can be fine-tuned as desired. Figure 3 shows the evolution of the measure ρ as a typical specimen progresses to the cracked regime from the initial uncracked regime. The predicted regime (using the thresholded approach) is shown along with the true (uncracked) regime which is generated from the microscope data. It is noted that the precursor in the cracked regime has no ground truth. The idea here is to be able to detect the imminent crack before it actually happens.

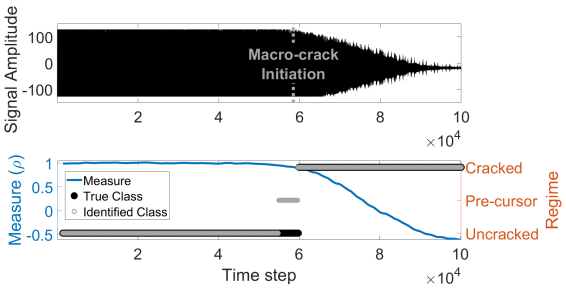

(a) Time-series #1: (Top) Signal and (Bottom) Measure (ρ)

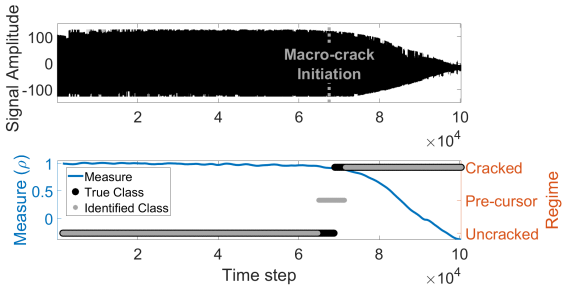

(b) Time-series #2: (Top) Signal and (Bottom) Measure (ρ)

Fig. 3: Measure (ρ) of two sample ultrasonic time-series, overlayed with the threshold-based regime prediction

Figure 3 shows that, for both time-series, the proposed algorithm is capable of detecting the emergence of cracks with good accuracy (e.g., $\sim 95\%$). Furthermore, the algorithm can detect an imminent crack ahead of its actual happening (e.g., $\sim 4,500$ time-steps ahead for Time-series #1 and $\sim 4,000$ time-steps ahead for Time-series #2). Thus, the proposed method *p-PFSA* is apparently useful for health monitoring of critical structural components without having to wait for a visible crack to appear.

6 Summary, Conclusions, and Future Work

This letter has reported the development and experimental validation of a novel fatigue crack detection method, called *p-PFSA*, which is data-driven and is capable of discriminating between uncracked and cracked regimes of mechanical structures before the appearance of a visible crack. The underlying algorithm is built upon the concept of projection-based probabilistic finite state automata (PFSA) and quantifies the emergence of imminent crack damage in terms of a signed measure. The efficacy of the proposed *p-PFSA* is demonstrated on a fatigue testing apparatus using cold-rolled AL7075-T6 specimens.

While there are many areas of research to enhance the work reported here, the following topics are suggested to be conducted in the near future:

1. Performance comparison of *p-PFSA* with other data-driven methods (e.g., hidden Markov modeling (HMM) and artificial neural networks (ANN)).
2. Verification of *p-PFSA* with additional experimental data, where knowledge of micro-crack emergence is available.

Acknowledgements

The authors are grateful to Dr. Najah F. Ghalyan and Dr. Eric E. Keller who have kindly provided the experimental data. The work reported in this paper has been supported in part by U.S. Air Force Office of Scientific Research (AFOSR) under Grant No. FA9550-15-1-0400 in the area of dynamic data-driven application systems (DDDAS). The work is also supported in part by Mechanical Engineering Department of Pennsylvania State University, University Park, PA 16802.

References

[1] Suresh, S., 1998. *Fatigue of materials*. Cambridge University Press, Cambridge, England.

[2] Ciang, C. C., Lee, J.-R., and Bang, H.-J., 2008. "Structural health monitoring for a wind turbine system: a review of damage detection methods". *Measurement Science and Technology,* **19**(12), p. 122001.

[3] Papazian, J. M., Nardiello, J., Silberstein, R. P., Welsh, G., Grundy, D., Craven, C., Evans, L., Goldfine, N., Michaels, J. E., Michaels, T. E., et al., 2007. "Sensors for monitoring early stage fatigue cracking". *International Journal of Fatigue,* **29**(9-11), pp. 1668–1680.

[4] Gupta, S., and Ray, A., 2007. "Real-time fatigue life estimation in mechanical structures". *Measurement Science and Technology,* **18**(7), p. 1947.

[5] Ghalyan, N. F., and Ray, A., 2020. "Symbolic time series analysis for anomaly detection in measure-invariant ergodic systems". *Journal of Dynamic Systems, Measurement, and Control,* **142**, June, p. 061003 (1 to 11).

[6] Mukherjee, K., and Ray, A., 2014. "State splitting and merging in probabilistic finite state automata for signal representation and analysis". *Signal Processing,* **104**, pp. 105–119.

[7] Ray, A., 2004. "Symbolic dynamic analysis of complex systems for anomaly detection". *Signal Processing,* **84**(7), pp. 1115 – 1130.

[8] Rajagopalan, V., and Ray, A., 2006. "Symbolic time series analysis via wavelet-based partitioning". *Signal Processing,* **86**(11), November, pp. 3309–3320.

[9] Bhattacharya, C., and Ray, A., 2020. "Online discovery and classification of operational regimes from an ensemble of time series data". *Journal of Dynamic Systems, Measurement, and Control,* **142**(11), 07.

[10] Berman, A., and Plemmons, R., 1994. *Nonnegative Matrices in the Mathematical Sciences*. SIAM, Philadelphia, PA, USA.

[11] Pastor, D., and Nguyen, Q.-T., 2013. "Random distortion testing and optimality of thresholding tests". *IEEE Trans. Signal Processing,* **61**(16), pp. 4161 – 4171.

[12] Poor, H., 1994. *An Introduction to Signal Detection and Estimation*. Spriger-Verlag, New York, NY, USA.